Journal of Applied Polymer Science

Properties of Insulin–Chitosan Complexes Obtained by an Alkylation Reaction on Chitosan

Emmanuel Robles,[1] Josué Juárez,[2] María. G. Burboa,[3] Luis E. Gutiérrez,[3] Pablo Taboada,[4] Víctor Mosquera,[4] Miguel A. Valdez[2]

[1]Departamento de Investigación en Polímeros y Materiales, Universidad de Sonora, Rosales y Transversal, Hermosillo 83000, Sonora, México

[2]Departamento de Física, Universidad de Sonora, Rosales y Transversal, Hermosillo 83000, Sonora, México

[3]Departamento de Investigaciones Científicas y Tecnológicas, Universidad de Sonora, Rosales y Transversal, Hermosillo 83000, Sonora, México

[4]Laboratorio de Física de Coloides y Polímeros, Grupo de Sistemas Complejos, Departamento de Física de la Materia Condensada, Facultad de Física, Universidad de Santiago de Compostela, Santiago de Compostela 15782, Spain

Correspondence to: M. A. Valdez (E-mail: miguel.valdez@correo.fisica.uson.mx)

ABSTRACT: In this study, we investigated the influence of hydrophobized chitosan on the formation and thermodynamic and surface tension properties of insulin–chitosan (I–Ch) polyelectrolyte complexes (PECs). We used an alkylation procedure to insert 12 carbon chains along the chitosan macromolecule with final substitution degrees of 5, 10, and 50%. NMR and IR spectroscopy were used to evaluate the success and extent of the hydrophobization procedure. Isothermal titration calorimetry (ITC) was used to determine the type and extent of the existing intermolecular interactions between the different constituting components of the insulin–hydrophobized chitosan PECs. Through the surface tension and diffusion coefficients at the air–water interface and ITC experiments with different I–Ch proportions, we demonstrated that around 34, 24, 25, and 60–80 insulin molecules saturated 0, 5, 10, and 50% hydrophobized chitosans, respectively. Surface tension experiments at the air–water interface demonstrated that the interaction of insulin molecules on the unmodified chitosan increased the hydrophobicity; this was mainly due to electrostatic interaction. On the contrary, insulin–hydrophobized chitosan interaction lowered the PEC hydrophobicity because of insulin alkyl chain interaction, and therefore, the hydrophilic insulin groups at the PEC surface contributed to a higher surface tension. © 2013 Wiley Periodicals, Inc. J. Appl. Polym. Sci. **2014**, *131*, 39999.

KEYWORDS: adsorption; drug-delivery systems; hydrophilic polymers; polyelectrolytes; proteins

Received 24 June 2013; accepted 24 September 2013

DOI: 10.1002/app.39999

INTRODUCTION

The properties of biopolymers have been studied a long time because of to their wide applications in the food, pharmaceutical, and cosmetic industries.[1] Several researchers have used biopolymers and synthetic polymers to optimize the load and release of bioactive molecules to increase their efficacy and therapeutic effect, lower the barriers of tissues and cells, and so on.[2] In particular, biopolymers are suitable materials as nanoparticles for medical applications because of their excellent biocompatibility and biodegradability and low immunogenicity.[3]

Chitosan is a cationic polysaccharide (pK_a ~6.5) obtained by the partial deacetylation of chitin, which is extracted from shells of crustaceans and some mushrooms.[4] Chitosan is biodegradable, nontoxic, and biocompatible.[5] In this way, chitosan is a good candidate for the preparation of nanocarriers for the transport and delivery of a wide range of drugs and biological agents, such as insulin, that can be protected along the superior gastric system (esophagus and stomach) until they reach the intestinal hilum, where they can be absorbed into the bloodstream.[3,6,7] Also, chitosan is a natural mucoadhesive and can bind to the intestinal mucosa and improve the residence time of drugs in the body.[8] However, insulin shows a low association with chitosan and then poor bioavailability.[9] This affects the capability of the chitosan nanoparticle to maintain stable glucose levels in the bloodstream. This problem can be overcome by the use of polymeric hydrogels or polymers with amphipathic properties, which improve the interaction with the protein and the ability of chitosan to bind to the intestinal wall cells.[10,11] Because insulin and amphiphilic polymers both possess hydrophobic and hydrophilic segments, it is expected that

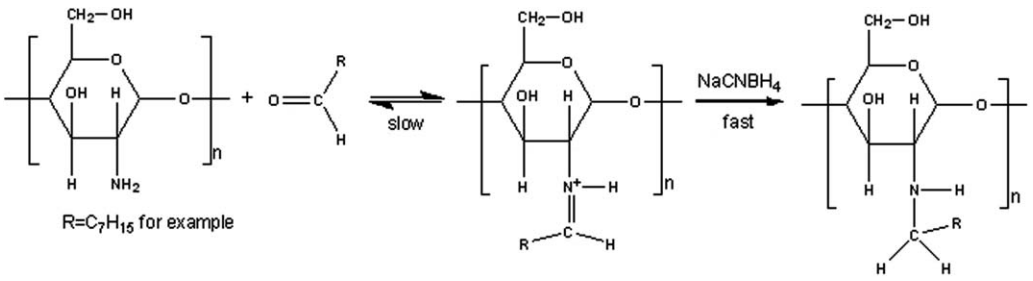

Figure 1. Diagram of the alkylation reaction on chitosan.

they will be mutually compatible and may be advantageous to the efficacy of drug association with the drug–polymer complex.

There have been many studies of insulin carriers based on different amphiphilic molecules, such as phospholipids, block copolymers (including pH-responsive hydrogels), responsive thermal gels, and time-degradable hydrogels.[10–14] The goal of investigations on these carrier systems has been to improve the release profile of insulin (*in vitro* or *in vivo*), increase the time range of insulin bioactivity, and decrease their possible cytotoxic effects. For instance, liposomes, one of the most studied carrier particulate systems, have shown potential for enhancing the oral bioavailability of protein and peptides. Specifically, liposomes, built up with sodium glycocholate in the liposomal formulation, have been used to enhance the bioavailability of insulin. In this regard, in *in vitro* assays and diabetic rat models, bilosomes have shown great insulin protection effects against enzymatic degradation and a high biodisponibility of the protein molecules.[12–14] However, studies on the interaction nature of insulin–polyelectrolyte complexes (PECs) have demonstrated the possible conformational alteration of the insulin structure upon its incorporation into such polymeric vehicles.[15,16]

The investigation of PECs (proteins, polysaccharides, and synthetic polymers) with drugs has increased in recent years. In aqueous media, PEC formation leads to stable nanoparticles that have the advantage of not needing organic solvents or sonication for preparation; this minimizes drug damage.[15] Analysis of the drug–PEC interaction is needed to understand the kind of interactions involved and to optimize the interaction with cells and biological tissues.[17] Several methods have been used to investigate ligand–protein, DNA–polysaccharide, and other interactions; some of these methods require laborious and sophisticated sample preparation.[18–22]

For a long time, surface tension measurements have been widely used to investigate protein–small organic molecules.[23] Even though this method is simple and can provide some qualitative knowledge about the interactions, we cannot determine the binding ratio between the two molecules. Interactions between PECs and different molecules induce surface changes, which can be measured by surface tension. Because the surface tension changes need only small amounts of surface-active materials, small quantities can be used efficiently compared to some methods for the measurement of the bulk properties. For instance, Yang et al.[17] showed that the molecular binding ratio between two different proteins could be determined from the measurement of the equilibrium surface tension as a function of their relative concentration.

In a previous study, we investigated the properties of nanoparticles of insulin–hydrophobically modified chitosans in the presence of sodium tripolyphosphate as a crosslinking molecule. The influence of different proportions of hydrophobic chains with 8, 10, and 12 carbons added to chitosan was used to observe improvements on *in vitro* insulin-release experiments.[9]

In this study, we investigated the interaction of insulin with unmodified chitosan (Ch) and hydrophobized chitosans chemically bound with a 12-carbon hydrophobic group. To assess the interactions, insulin was incorporated into the same polymeric formulation, and the diffusion coefficients at the air–water interface (D_{a-w}'s), the adsorption at the lag time (LT) of the insulin–PECs, and isothermal titration calorimetry (ITC) results were compared to understand the effect of the hydrophobicity on the interaction of insulin and chitosan and to estimate the insulin–chitosan (I–Ch) molecular proportion on the insulin–PECs. Dynamic light scattering (DLS) was used to measure the average sizes of the PECs, and NMR and IR spectroscopy were used to demonstrate the hydrophobic chain bonded to the chitosan molecule.

EXPERIMENTAL

Materials

Chitosan with an average molecular weight of 415,000 g/mol and a 90% degree of deacetylation was purchased from Fluka (catalog number 28,191, middle-viscosity grade). Sodium cyanohydroborate ($NaCNBH_4$), dodecyl aldehyde, and insulin (human recombinant, 1 mg equivalent to 29.1 USP units) were purchased from Sigma-Aldrich Co. and were used as received. Water was filtered with an Easy Pure/Barnstead instrument with a resistivity of 18.2 MΩ cm. All organic solvents were High Performance Liquid Chromatography grade, and all other chemicals were reagent grade.

Synthesis of the Hydrophobized Chitosan

The hydrophobization of chitosan was done by a reductive amination reaction according to a procedure described in the literature.[24] This method produces a covalent bond between a reactive substrate and the amine group of chitosan (see Figure 1). The reactive substrates in this study were 12-carbon hydrocarbon chains. The alkylation reaction was as follows: 2 g of chitosan was dissolved in 110 mL of acetic acid (0.2*M*). After complete dissolution, 75 mL of ethanol was added to allow the aldehyde to be in a solvating medium. The pH was adjusted to 5.1 to prevent the precipitation of chitosan. A corresponding aldehyde proportion (5, 10, or 50%) was diluted in ethanol and added to the chitosan solution; thereafter, an excess of sodium

cyanohydroborate (3:1 mol/mol chitosan) was added. The mixture was stirred for 24 h at room temperature, and the alkylated chitosan was precipitated with ethanol. Then, the pH was adjusted to 7, and the precipitate was washed several times in ethanol–water mixtures of increasing ethanol contents from 70 to 100% v/v. In this manner, we synthesized a variety of hydrophobic chitosans by keeping the length of the hydrophobic chain constant (at 12 carbons) and varying the substitution degree along the chitosan backbone (5, 10, and 50%). For future reference, these batches were named Ch, ChA (5%), ChB, (10%), and ChC (50%) for the unmodified chitosan and the three different hydrophobized chitosans, respectively.

DLS

DLS measurements were performed with an ALV-5000 digital correlator system (ALV 5000/E, ALV GmbH, Germany) fitted with a temperature control set to 25 ± 0.1°C. The scattered light was vertically polarized with a solid-state laser (2 W, 488 nm wavelength). The hydrodynamic radius (R_H) was obtained for the diluted samples from DLS measurements at an incidence angle of 90° by analysis of the DLS data with the CONTIN algorithm developed by Provencher and the application of the Stoke–Einstein equation:

$$R_H = K_B T / 6\pi\eta D_0$$

where K_B is the Boltzmann constant, T is the absolute temperature (K), η is the solution viscosity, and D_0 is the bulk diffusion coefficient of the particles in solution. Measurements were performed in triplicate with a sampling time of 120 s each and averaged.

Fourier Transform Infrared (FTIR) Spectroscopy

IR spectra were acquired with an FTIR instrument (Perkin Elmer, model Spectrum GX) coupled to a PC. The samples were freeze-dried and mixed with KBr pellets in the sample holder, which was placed directly in the trajectory of an IR laser beam. The transmittance was observed for the mid-IR range of 500–4000 cm^{-1}. The IR spectra were collected 16 times (spectral resolution = 1 cm^{-1}) and were analyzed with Spectrum software.

^{1}H-NMR Spectroscopy

High-resolution ^{1}H-NMR spectra were recorded on a Bruker (Avance, 400 MHz) spectrometer. An amount of 5 mg of different samples was dissolved at 40°C in 0.5 mL of 2% v/v DCl–D_2O (1%, pH 4). All of the spectra were recorded at 300 K.

ITC

ITC measurements were performance on a VP-ITC ultrasensitive titration calorimeter from MicroCal, Inc. (Northampton, MA) with a sample cell volume of 1.436 mL at 25°C. All of the solutions were thoroughly degassed before use by magnetic stirring *in vacuo*. The sample cell was loaded with a cationic chitosan solution (8×10^{-4} m*M*) dissolved in acetate buffer (10 m*M*, pH 4.8), and the reference cell was filled with pure buffer solution. The syringe was filled with an anionic insulin solution (0.68 m*M*) dissolved in NaOH (0.01*M*, pH 9.2) and was introduced into the thermostat cell. The solution in the cell was stirred at 350 rpm by a syringe equipped with a micropropeller to ensure rapid mixing and prevent foaming on the solutions. The titration of the protein with the biopolymer involved 11 consecutive injections of the insulin solution, the first being 2 μL (neglected in the analysis) and the remaining ones being 12 μL. In all cases, the injections were started after the baseline stability had been achieved and were programmed to occur at 200 s intervals. Control experiments were carried out, in which identical aliquots were injected into the buffer solution, to correct for the thermal effects due to the biopolymer solution. All of the experiments were carried out in duplicate, and the reproducibility was within ±3%. The data were collected automatically and subsequently fitted to a sigmoidal function (dose–response) carried on the Origin 7.0 microCal ITC software supplied by the manufacturer. After the heat of control dilution was subtracted, a nonlinear least squares algorithm (minimizing Chi squared) along with the concentrations of the titrant (insulin, in our case) and the samples (chitosan solutions) were used to fit the heat flow per injection to an equilibrium binding equation and provide the best fits for the values of stoichiometry (n), the binding constant (K_b), and the change in enthalpy (ΔH).

Surface Tension and Rheology Measurements

Drop tensiometry was used to determine the dynamic interfacial tension (γ) and the interfacial dilatational rheology measurements at the air–water interface with the air bubble in the upward direction. The bubble was formed at the tip of a U-shaped stainless steel needle (0.5-mm inside diameter) immersed in the aqueous I–Ch solutions contained in a quartz cuvette (103.051 F-Og, 20-10, Hellma, Germany). The equipment used was a Tracker tensiometer (I. T. Concept, France) capable of real-time surface tension measurements with accuracy of 0.1 mN/m. Measurements of γ and the rheological measurements were based on the digital profile of the drop image and the solution of the Gauss–Laplace equation. The software used for the axisymmetric drop shape analysis was Win Drop software (I. T. Concept, France). The temperature was kept constant at 25 ± 0.1°C.

Two chitosan concentrations were used (8×10^{-5} and 8×10^{-4} m*M*), and different insulin–polymer mixtures were prepared from insulin solutions (0.068 and 0.68 m*M*, respectively) to obtain different insulin–polymer molar ratios from 1 to 115. The chitosan solutions, insulin solutions, and mixtures were prepared in the same way described for the ITC method to correlate the results.

For the analysis of γ, dilatational elastic modulus (E'), and viscous modulus (E'') at the air–water interface, measurements were started after the absolute value of $d\gamma/dt$ was lower than 0.01. The used frequencies (ωs) were 0.05, 0.07, 0.1, 0.25, 0.5, 0.76, and 1 s^{-1}. Both rheological parameters were measured by the oscillation of drops with a 10% maximum drop volume increment. All of the measurements were repeated at least three times, and the chitosan concentration used was kept constant (8×10^{-4} m*M*).

THEORY

Sinusoidal Perturbations of Interfaces with a Drop Tensiometer

For a given sinusoidal drop pulsation of ω produced by the Tracker tensiometer at every time (t), we obtained a surface tension value [$\gamma(t)$] by analyzing the axial symmetric shape of the pendant drop and the drop area [$A(t)$], which were used to

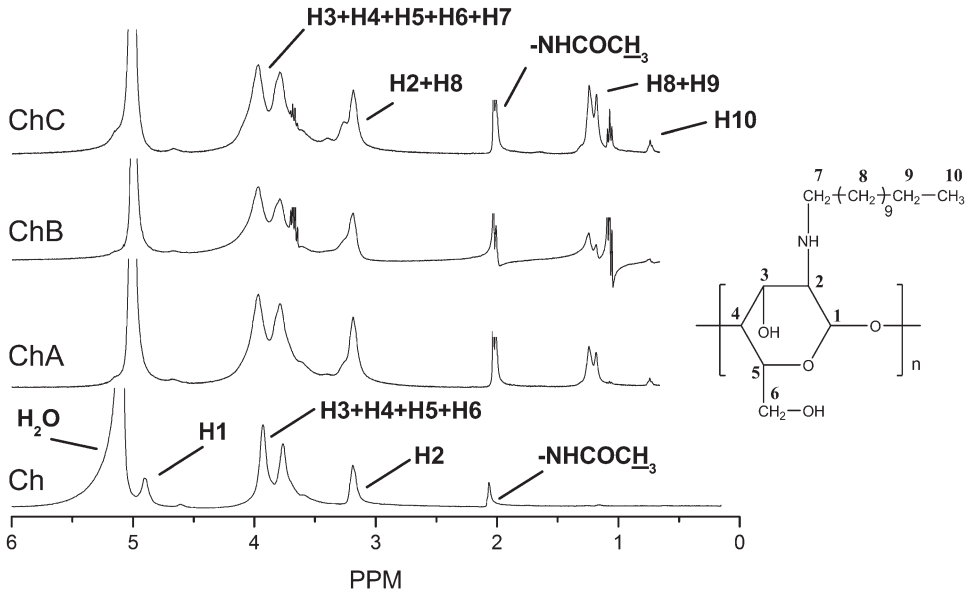

Figure 2. [1]H-NMR spectra of Ch, ChA, ChB, and ChC.

calculate the complex dilatational elasticity modulus (E), defined as follows:

$$E = -A\frac{d\gamma}{dA} \tag{1}$$

where A refers to the area occupied by one molecule at the air–water interface and γ is the surface tension (mN/m). E can also be defined as a complex function, which can be written as follows:

$$E = E'(\omega) + iE''(\omega) \tag{2}$$

where $E'(\omega)$ and $E''(\omega)$ correspond, respectively, to the real and the imaginary parts of the viscoelastic modulus.[25] They are related to the changes in $\gamma(t)$ and $A(t)$ in the interface by eq. (1) and with the phase angle (ϕ) between $d\gamma(t)$ and $dA(t)$. The real and imaginary parts are related to the complex modulus by $E' = E\cos(\phi)$ and $E'' = E\sin(\phi)$, respectively. If the phase difference approaches zero, the surfaces can be considered elastic; otherwise, the surface shows viscoelastic behavior.[26] With the assumption that the mechanical properties of the interface follow the Maxwell model, the elastic (storage) part in eq. (2) is represented by

$$E'(\omega) = E'_0 + \Delta E'\frac{\omega^2\tau^2}{1+\omega^2\tau^2} \tag{3}$$

The viscous (loss) part is written as follows:

$$E''(\omega) = \Delta E''\frac{\omega\tau}{1+\omega^2\tau^2} \tag{4}$$

where E_0' is the extrapolated value of the elastic modulus at the limit $\omega = 0$, $\Delta E'$ and $\Delta E''$ are the real and imaginary parts contributions of the viscoelastic modulus at infinite frecuencies, respectively and τ is the relaxation time characteristic of the Maxwell model.[27] We found the last two parameters by fitting the experimental values with the Levenberg–Marquardt nonlinear least squares minimization routine in OriginPro 8.0 (Northampton, MA), adjusting the parameters given in eqs. (3) and (4). The short time diffusion of proteins at the air–water interface can be approached by the asymptotic solution for $t \to 0$ of the diffusion coefficient, described by Miller, which is given by

$$D_{a-w} = \frac{\pi}{4}\left[\frac{1}{RTC_0}\left(\frac{d\gamma}{d\sqrt{t}}\right)_{t\to 0}\right]^2 \tag{5}$$

where D_{a-w} is the diffusion coefficient near the air–water interface (m^2/s), R is the universal gas constant (J mol^{-1} K^{-1}), C_0 is the bulk protein concentration (mol/m^3), and t is the time (s).[28]

The behavior in the region time $t \to \infty$ of the function γ versus $t^{1/2}$ was obtained with the assumption of a diffusion-controlled adsorption and is given by the Joos relationship:[29]

$$\gamma - \gamma_\infty = \frac{RT\Gamma^2}{2C_0}\left(\frac{\pi}{D_0 t}\right)^{1/2} \tag{6}$$

where γ_∞ is the extrapolated equilibrium interfacial tension at $t \to \infty$ and Γ is the excess concentration of protein molecules at the surface at long times.

The size of the insulin and insulin–PECs was estimated at short times via the following equation:

$$r = \sqrt{\frac{1}{\Gamma_m h\pi^3}} \tag{7}$$

where r is the radius of the assumed circular cross section of the molecule at the interface, Γ_m is the excess concentration of protein molecules at the surface at LT, and h is Avogadro's constant.[17]

RESULTS AND DISCUSSION

Spectroscopy of the Modified Chitosans

We used [1]H-NMR and FTIR spectroscopy to check the success of the hydrophobization of the chitosan chain, the substitution of the hydrophobic molecules, and the degree of substitution.

[1]H-NMR Spectroscopy

The [1]H-NMR spectra of the chitosan and modified chitosan are given in Figure 2. The [1]H-NMR assignment of chitosan was as follows: H1 $\delta = 4.2$ ppm; H2 $\delta = 2.6$–2.8 ppm; H3, H4, H5,and

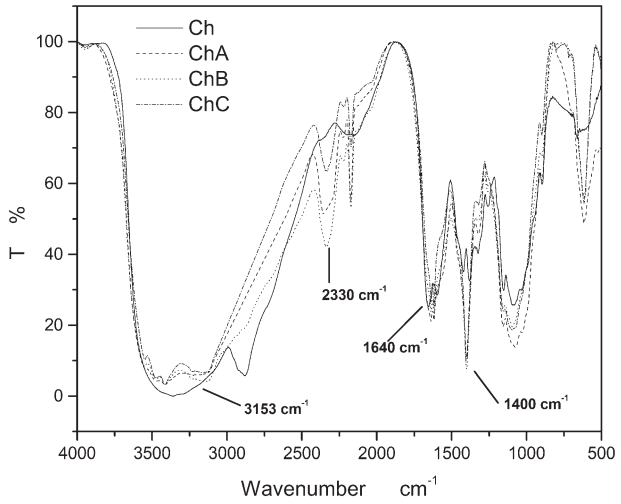

Figure 3. FTIR spectra of Ch, ChA, ChB, and ChC.

H6 $\delta s = 3.3–3.5$ ppm; and $NHCOCH_3$ $\delta = 1.6$ ppm.[30–32] The shape of H1 was affected by the near D_2O peak inhibition spectra at $\delta = 4.7$ and the protons of the glucosamine and *N*-acetyl glucosamine residues from partially deacetylated chitosan. The others were assigned to the aliphatic chain of the aldehyde molecule [$\delta = 1.1$ (H8 and H9) and $\delta = 0.6$ (H10) ppm]. The intensities of the latter peaks increased in direct proportion to the degree of substitution. The integral of each of the peaks allowed us to calculate the degree of substitution of the hydrophobized chitosan. We performed a microanalysis of the NMR experimental data obtaining the following proportions of the hydrophobic substituents: 5.4, 4.6, 10.9, and 53.1% for the Ch, ChA, ChB, and ChC samples, respectively.[9]

FTIR Spectroscopy

The FTIR spectra of Ch and the modified chitosans are shown in Figure 3. The broad band located between 4000 and 2800 cm^{-1} was associated with the stretching of —NH_2 and —OH groups. From the Ch spectrum, we found that distinctive absorption bands appeared at 1662 cm^{-1} (amide I), 1605 cm^{-1} (—NH_2 bending), and 1393 cm^{-1} (amide III). The absorption bands at 1164 cm^{-1} (asymmetric stretching of the C—O—C bridge), 1092 cm^{-1}, and 1042 cm^{-1} (skeletal vibration involving the C—O stretching) were characteristic of the saccharine structure.[33] Compared with that of Ch, the IR spectra of the modified chitosans showed that a new signal at 1640 cm^{-1} and a weak absorption at 2330 cm^{-1}, which were assigned to the amino group vibration. In addition, the peak at 1605 cm^{-1} was attributed to a decrease in the unreacted amino groups; this indicated that the amino group of Ch was partly substituted by the aldehyde molecules via the amino bond.

Thermodynamic Analysis with the ITC Data

We present the results of the ITC experiments in terms of the heat of injection normalized by the insulin concentration added per each injection (Q^*) as a function of the I–Ch molar ratio after the subtraction of background titration. Figure 4 shows the ITC curves of Ch and the three different hydrophobized chitosans for different I–Ch molar proportions (final solution pH $\approx$ 5.3). As shown in Figure 4, we observed that the protein–chitosan interaction was an exothermic process, and the thermal equilibrium was not reached at these titration values. The local heat increase for low I–Ch molar ratios was caused by electrostatic interaction, where the cationic biopolymer was expected to be in excess in comparison with the anionic protein molecule. This effect was accentuated in the case of the I–Ch complex, which held a higher number of available cationic sites or nonhydrophobized amine groups. Meanwhile, the complexes formed with ChA and ChB showed an absolutely larger value of the exothermic heat upon the first injection of insulin than the complex formed with ChC. This behavior should have been caused by the presence of the hydrophobic substituents on the modified chitosans, where the aliphatic chain tended to avoid exposure with the solvent; this caused a surface exposition of the residual cationic charge to the solvent, which enhanced the electrostatic interactions with insulin. This idea was also supported by a faster complexation, which was denoted by the presence of the exothermic minima at lower I–Ch molar ratios. On the other hand, ChC, with a higher degree of substitution, enabled progressive bounding with insulin (Figure 4), where the maximum *n* value was reached by this complex (see Table I). In this case, both electrostatic and hydrophobic interactions were present; this caused the observed shift in the exothermic minimum to larger I–Ch molar ratios, and the decrease in the released heat values showed that the hydrophobic interactions were slightly endothermic, with energies in the range of 2 kcal/mol.[34]

The sharp evolution of all plots to markedly lower the exothermic values with the further addition of insulin revealed a strong structural change in the system, most likely related to the substituent present on the modified chitosan. This complex formation between the charged protein and polysaccharides caused structural changes to both components of the complex at the molecular level.[35] These structural changes were related to the

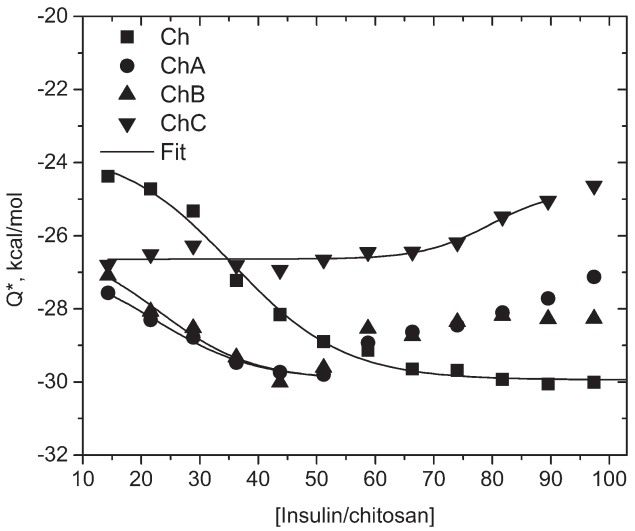

Figure 4. ITC data from the titration of 0.68 m*M* insulin in the presence of four different kinds of chitosan (8×10^{-4} m*M*): heat evolved per mole of insulin added versus the I–Ch molar ratio for each injection. The data were fitted to a dose–response binding model. The symbols represent the experimental data, and the lines represent the best fit.

Table I. Thermodynamic Parameters of Interaction for Insulin with the Unmodified and Hydrophobized Chitosans

Sample	*n*	$K_b \times 10^2$ (M^{-1})	ΔH (kcal/mol)	ΔG (kcal/mol)	$T\,\Delta S$ (kcal/mol)
I-Ch	35.5 ± 1.9	1.66 ± 0.1	−6.34 ± 0.4	−3.03	−3.31
I-ChA	22.1 ± 2.5	1.17 ± 0.2	−3.30 ± 0.4	−2.82	−0.47
I-ChB	23.1 ± 3.1	0.95 ± 0.2	−3.72 ± 0.5	−2.71	−1.01
I-ChC	79.7 ± 4.1	0.81 ± 0.3	−1.91 ± 0.2	−2.61	0.70

K, binding equilibrium constant; ΔG, free energy change.

aggregated complexes, which produced endothermic signals due to water molecule delocalization around the forming complex and the release of counter ions from residual charges along the polyelectrolyte chain, which were not neutralized during the first bending phase.[36,37]

Thermodynamic Parameters of the Insulin–PEC Interactions

ITC is a sensitive technique, where the summation of the heat effects determine the shape of the binding isotherm. These effects include the dilution of both host and ligand molecules in the system, in particular, chitosan and insulin, and the condensation and aggregation of the macromolecules. Also included are effects of coupled protonation and possible conformational changes upon binding.[38] With the aim of evaluating the I–Ch interactions and understanding the formation of our PECs, we conducted the thermodynamic analysis by fitting only the first binding stage (after the minima exothermic value was reached). We believe that the second binding stage was dominated by electrostatic and hydrophobic interactions, which caused conformational changes on the PECs. The best fit for the integrated heat was obtained, and the thermodynamic parameters are shown in Table I. Because the ITC measurements of the interaction of insulin with the different chitosans were obtained under identical conditions, a direct comparison of the thermodynamic parameters between them was possible. As observed from Table I, insulin bonded more tightly to Ch than to the hydrophobized chitosan; this difference quantitatively caused an additional change in the free energy of about 0.42 kcal/mol (compared to ChC); this reflected a higher stability of Ch. Also, the data indicate that the I–Ch binding was more exothermic (−6.34 kcal/mol) in comparison with I–ChA (−2.82 kcal/mol). Although the binding reaction was mostly enthalpically driven, the results show an increased value in the entropy change (ΔS) for all of the insulin–hydrophobized chitosan PECs in comparison with the corresponding ΔS value of the I–Ch PEC; this indicated that the binding was favored by an increase in the conformational entropy. This led us to think that a large number of hydrophobic substituents in I–ChC caused the system to be enthalpically favored and entropically driven by the conformational reorganization of the macromolecule structure among the solvent and the complex. Finally, the *n* value found for the I–Ch PEC was in accordance with the I–Ch ratios obtained with low-molecular chitosans by Lee et al.[39]

Interfacial Diffusion and Surface Tension at Short Times

We investigated the absorption of insulin and I–Ch PECs for different molar proportions at the air–water interface in the convection and diffusive limit regimes with the drop tensiometer. As shown in Figure 5, we obtained the behavior of LT of the I–Ch complexes for different I–Ch molar ratios. The chitosan concentration used was 8×10^{-5} m*M*, which was low enough to observe the lag behavior of the surface tension. LT, during which the surface pressure is very low, is characteristic of protein adsorption curves.[40] It is obtained as the intersection between the time axis and the straight line following the beginning of the pressure increase and corresponds to the diffusive regime of the molecular absorption. LT represents the conventional boundary between the gaseous and liquid-extended regimes of the adsorption layers.[41] We observed the known behavior in the convention limit (very low concentration of proteins) and the concentration behavior in the diffusion limit (higher concentrations), which have also been observed by other researchers.[40–44]

As shown in Figure 5, we observed that for I–Ch ratios lower than 25, the insulin LT was larger than the LTs of all of the complexes; this indicated that for these insulin concentrations, insulin remain bound to the polymer chains and a higher interaction was produced between the I–Ch complexes at the interface in comparison with free insulin. Up to an I–Ch molar proportion of 25, the LT of insulin and the LTs of I–ChA and I–ChB showed almost the same values, and up to a molar proportion of 32, we observed that LT for the insulin and I–Ch complex had similar values; this means that from these insulin proportions, the corresponding insulin complexes reached saturation, and the insulin molecules remained free in solution,

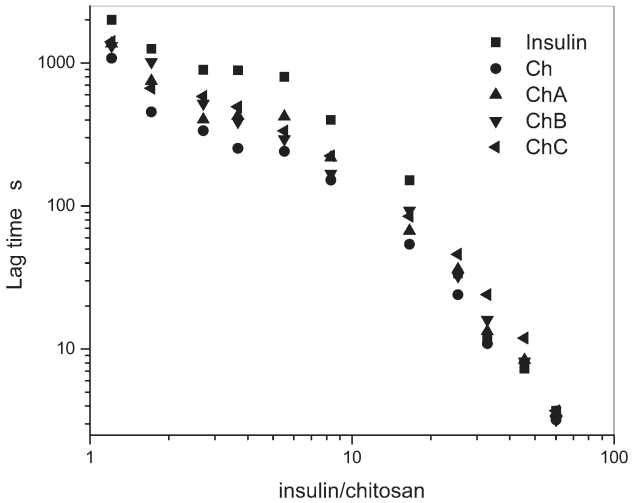

Figure 5. LT of the I–Ch complexes for different I–Ch molar proportions. The chitosan concentration used was 8×10^{-5} m*M* at 25°C.

Table II. Interfacial Average Radius (nm) of the Insulin and Insulin–PECs Used in This Study for Different I–Ch Molar Ratios Calculated at LT from the Ward Tordai Equation

I-Ch	Insulin	Ch	ChA	ChB	ChC
1.2	2.2	9.8	10.4	10.7	9.0
1.7	2.1	12.2	12.1	11.4	10.8
2.7	1.8	13.2	14.2	13.5	11.2
3.7	1.6	14.1	14	14.5	11.7
5.5	1.3	14.3	14.0	15.6	12.9
8.3	1.3	16.0	16.5	17.9	14.2
16.6	1.1	20.8	22.2	20.8	18.2
25.4	1.4	25.5	25.9	27.1	21.2
32.8	1.5	31.0	33.3	32.3	24.9
45.5	1.5	33.4	37.3	38.2	29.7
60.1	1.5	42.1	46.1	48.3	39.7

reaching the interface at the same time as free insulin. It was interesting to observe that insulin saturated the most hydrophobic chitosan (ChC) until a molar proportion near 60 was reached. This was in accordance with the results obtained for the high insulin association efficiency and load capacity of the nanoparticles built with this hydrophobic chitosan.[9] Comparing the results of n obtained in Table I, we observed very close values of the saturation molar proportions for I–Ch, I–ChA, I–ChB, and I–ChC with the corresponding binding sites obtained previously with the ITC method.

The behavior of the I–Ch (unmodified and hydrophobized) PECs at the air–water interface for different I–Ch proportions was analyzed at LT. With the Ward Tordai equation and the diffusion coefficients from DLS results, we obtained the average radii of the adsorbed insulin and insulin–PECs, modeled as a circle at the air–water interface [eq. (7)]. The average diffusion coefficients obtained by DLS for insulin were 8.8×10^{-11} m^2/s for Ch and 0.32, 0.20, 0.18, and 0.35×10^{-11} m^2/s for ChA, ChB, and ChC, respectively.[41]

As shown in Table II, we observed that the interfacial radius grew with the increase in insulin on the chitosan PECs. This means that as long as LT decreased (higher I–Ch ratios), the adsorption amount of the PEC was lower, but on the other hand, the size of the adsorbed PEC at the interface was larger.[41] The larger sizes of ChA, ChB, and Ch at this time (LT) in comparison with ChC indicated that the interaction with insulin was mainly electrostatic, increasing hydrophobic molecular groups at the PEC backbone and, therefore, increasing the average interfacial molecular radius. The smaller size observed for insulin at higher insulin concentrations (shorter LT) indicated that only part of the insulin molecule was adsorbed at the interface in comparison with the corresponding R_H of the insulin hexamer (2.7 nm).

We analyzed the behavior of the PECs in the diffusive regime after LT. As shown in Figure 6, we observed the behavior of the diffusion coefficients at the short times obtained with eq. (5). We noticed that for an I–Ch molar ratio lower than 4, the insulin–hydrophobic chitosan PECs showed a smaller diffusion coefficient than the I–Ch complex; this indicated that the formation of the insulin–hydrophobic chitosan complex was driven by hydrophobic and electrostatic interactions; meanwhile, the I–Ch PEC was mainly stabilized by electrostatic forces at this initial insulin concentration, as was also demonstrated by the ITC experiments. The interaction of insulin with Ch left insulin hydrophobic groups at the interface of the complex and solvent, and this contributed to greater diffusion near the air–water interface. In the range of 4–25 I–Ch molar proportions, all of the PECs behaved similarly; that is, the diffusion coefficients of the PECs were smaller than that of insulin for the same insulin concentrations. When the I–Ch molar proportion was higher than 25, we noticed that the I–ChA and I–ChB PECs had diffusion coefficients similar to that of free insulin; this means that at these molar proportions, these PECs were saturated and insulin remained unbound in the solution. This probably let the insulin molecules reach the interface at shorter times in comparison with insulin–hydrophobic chitosan complexes and at similar times as pure insulin. For the case of I–Ch PEC, this saturation was reached for a molar proportion around 34. Finally, the most hydrophobic I–ChC complex reached saturation at a molar proportion around 110. This complex probably needed more insulin molecules to saturate, as we demonstrated previously with the ITC analysis. However, in this case, the proportion of insulin on the ChC chitosan was higher than the ones calculated by LT measurements as was the number of binding sites calculated by the ITC experiments.

Interfacial Surface Tension and Rheological Behavior of the I–Ch and Insulin–Hydrophobic Chitosan PECs at Long Times

The behavior of the surface tension of the I–Ch PECs extrapolated *ad infinitum*, according to eq. (6), is shown in Figure 7 for different insulin concentrations. In aqueous media, the decreasing surface tension of the protein solutions in the presence of surfactants or different ligands has been observed by several researchers.[43,45] As shown in Figure 7, we observed that around a molar proportion of 11, all of the complexes reached

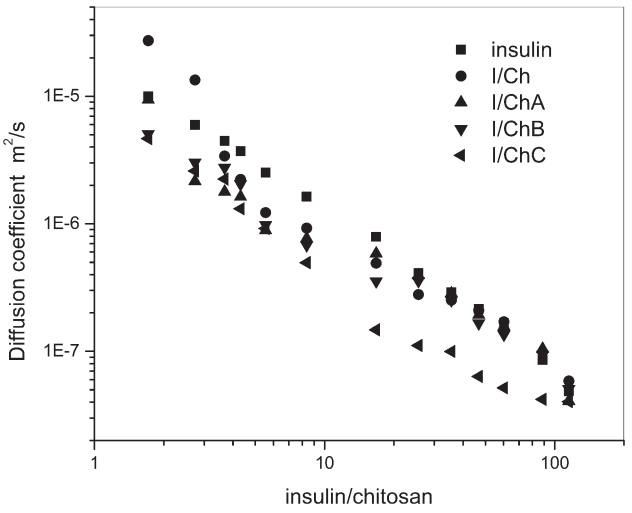

Figure 6. Behavior of D_{a-w} at short times of insulin–PECs for different I–Ch molar ratios at 25°C.

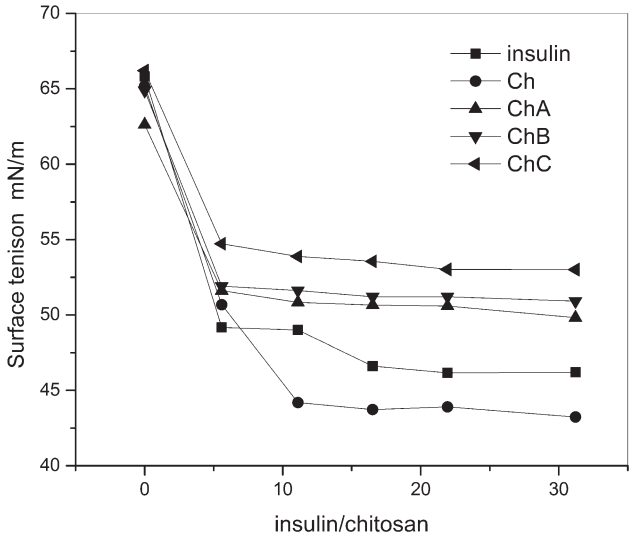

Figure 7. Extrapolated surface tension ($t \rightarrow \infty$) versus I–Ch molar ratios for insulin and all insulin–PECs used.

an almost constant surface tension, which practically did not change at higher insulin concentrations. Similarly, the surface tension of insulin reached a constant value around 46.2 mN/m. It was interesting to notice the effect of insulin on the long-time surface tension values of the different I–Ch PECs. I–Ch showed the lowest surface tension, including compared to that of pure insulin; this indicated that the hydrophobicity increased as mentioned previously, and therefore, the main interactions between insulin and nonmodified chitosan were electrostatic, in agreement with the ITC experiments and as also demonstrated by Robles et al.[9] According to the results of Figure 6, the I–Ch complex showed a bigger diffusion constant for low and moderate I–Ch proportions (<20) in comparison with insulin-modified chitosans. This behavior was also observed by other researchers.[46] This interaction left hydrophobic insulin amino acids at the interface and contributed to a lower surface tension.

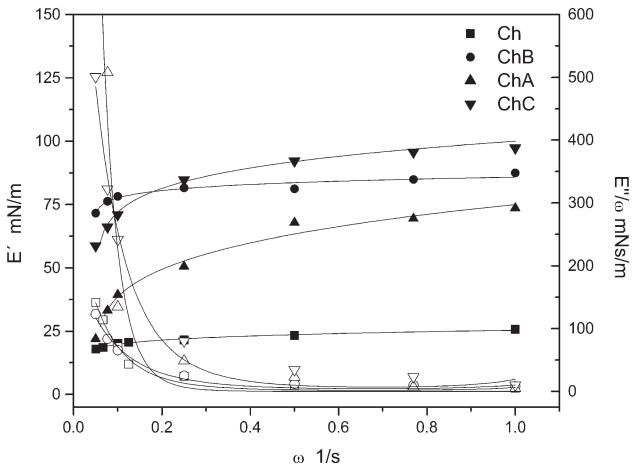

Figure 8. Real part of E' (filled symbols) and complex viscosity (E''/ω; empty symbols) versus the dilatational ω of the unmodified and hydrophobized chitosans in acetate buffer (pH 4.8) solutions (8×10^{-4} mM) at 25°C. The lines represent the best fit adjusted to Maxwell model.

Table III. Maxwell Model Values of E' (mPa) and Viscosity $\eta_{\omega \rightarrow 0}$ (mPa s) at Long Times at the Air–Water Interface and relaxation time τ (s); respectively for Chitosan, the Different Hydrophobized Chitosans, and Their Insulin Complexes with an Insulin–Chitosan Ratio of 30

Sample	$E_0 + \Delta E$ (mPa)	$\eta_{\omega \rightarrow 0}$ (mPa s)	t (s)
Ch	26.0 ± 1.0	141.6 ± 12	4.0 ± 0.2
ChA	70.4 ± 3.0	123.2 ± 6	4.5 ± 0.1
ChB	88.0 ± 1.0	501 ± 10	7.8 ± 1.0
ChC	95.8 ± 2.0	913.6 ± 15	8.3 ± 0.5
I-Ch	30.7 ± 2.1	84 ± 9.0	2.4 ± 0.4
I-ChA	40.8 ± 0.5	251.5 ± 10	8.7 ± 0.5
I-ChB	42.8 ± 1.0	320.0 ± 12	12.2 ± 1.0
I-ChC	45.4 ± 0.5	327.2 ± 15	11.9 ± 0.4

On the other hand, the insulin–hydrophobic chitosans showed a higher surface tension than insulin and the I–Ch PEC. This could have been due to the contribution of both electrostatic and hydrophobic interactions, which would have enhanced the presence of more hydrophilic insulin amino acids and hydrophilic chitosan sections at the complex–water interface and increased the surface tension; this was more noticeable for the chitosan modified with the highest hydrophobic proportion used. Correspondingly, the diffusion coefficient of I–ChC showed (Figure 6) the lowest value in almost the whole range of I–ChC proportions in accordance with the results of Perez et al.[47] Finally, in Figure 8, we show the behavior of the E' (real part) of chitosan and the different hydrophobic chitosans for different ωs. Also, the Maxwell model fit with eqs. (3) and (4) is shown for each sample. We observed that for higher ωs, an increase in the hydrophobicity produced higher E' values of the hydrophobic chitosans at the interface; this could have been due to higher interchain hydrophobic interactions; on the contrary, Ch produced a very flexible layer at the interface, probably because of the steric and electrostatic repulsion, in addition to desorption process from the air–water interface to the bulk phase.

In Table III, we summarize the behavior of E' extrapolated at higher ωs, the viscosity at low ωs, and τs for the different chitosans and the corresponding I–Ch complexes for the I–Ch proportion of 30 obtained according to the Maxwell model. Interestingly, we observed that both the viscosity and E' increased with the increase in the hydrophobic proportion in chitosan. τ also increased; this indicated that a longer time was needed for the hydrophobic chitosans to stabilize at the interface. On the contrary, Ch needed less time to stabilize at the interface; this was probably due to the stronger electrostatic interaction compared with the hydrophobic one. The E' values extrapolated at higher ωs decreased about 50% with the insulin interaction in comparison with the corresponding hydrophobized chitosan; on the contrary, the interaction I–Ch slightly increased the interaction at the interface. This decreased the electrostatic interaction and enhanced the hydrophobic interaction added by insulin. As explained previously (Figure 7), the presence of insulin in the most hydrophobized chitosan (ChC)

increased the electrostatic groups at the complex surface; this increased the interchain repulsion and, therefore, decreased E' and increased the surface tension. However, the hydrophobicity of the chitosans still dominated the interaction, and E' was higher for the I–ChC PEC than for the other insulin–PECs. Notice also that insulin produced a less viscous film and increased τ for all of the hydrophobic chitosans because of the screening of the hydrophobic interchain interactions. On the contrary, τ for the I–Ch complex was lowered because of the increase in the hydrophobic interaction at the interface.

CONCLUSIONS

We modified chitosan with 12-carbon hydrocarbon tails with different proportions (5, 10, and 50%) and characterized the I–Ch PECs. With D_{a-w} and LT measurements at the air–water interface of the I–Ch and insulin–hydrophobized chitosans PECs, to compare their behavior with the ITC experiments, we observed a close relationship between the K_b values deduced from the ITC experiments and the I–Ch molar proportions of the corresponding PECs, where both the diffusion coefficients and LT values were more or less coincident with the ones of pure insulin (ca. 34 for I–Ch, 25 for both I–ChA and I–ChB and 70 for I–ChC). We also found that the main interaction of insulin with Ch was electrostatic at low and moderate I–Ch proportions. On the contrary, hydrophobically modified chitosan presented both electrostatic and hydrophobic interactions, and as long as the hydrophobicity of the chitosan increased, the interaction with insulin was mainly hydrophobic; this left a higher hydrophilic insulin residue proportion at the insulin–PEC surface, which produced a higher surface tension at the air–water interface in comparison with insulin and the other PECs analyzed.

ACKNOWLEDGMENTS

One of the authors (E.R.) acknowledges Consejo Nacional de Ciencia y Tecnología (CONACyT; México) for the doctoral scholarship and the Department of Research of Polymers and Materials of University of Sonora, México. Another author (M.A.V.) is grateful for the financial support of CONACyT for the sabbatical leave at the University of Santiago de Compostela, Spain (contract grant number 151794). The authors also acknowledge the support of the research group of the Laboratory of Colloid Physics and Polymers of Universidad de Santiago de Compostela, Spain.

REFERENCES

1. Yang, Y.; Anvari, M.; Pan, C.-H.; Chung, D. *Food Chem.* **2012**, *135*, 555.
2. Nitta, S. K.; Numata, K. *Int. J. Mol. Sci.* **2013**, *14*, 1629.
3. Wong, T. W. *Recent Pat. Drug Delivery Formul.* **2009**, *3*, 8.
4. Roberts, G. A. F. Chitin Chemistry; MacMillan: London, **1992**.
5. Gan, Q.; Wang, T.; Cochrane, C.; McCarron, P. *Colloids Surf. B* **2005**, *44*, 65.
6. Gan, Q.; Wang, T. *Colloids Surf. B* **2007**, *59*, 24.
7. Ieva, E.; Trapani, A.; Cioffi, N.; Ditaranto, N.; Monopoli, A.; Sabbatini, L. *Anal. Bioanal. Chem.* **2009**, *393*, 207.
8. Prego, C.; Garcia, M.; Torres, D.; Alonso, M. J. *J. Controlled Release* **2004**, *101*, 151.
9. Robles, E.; Villar, E.; Alatorre-Meda, M.; Burboa, M. G.; Valdez, M. A.; Taboada, P.; Mosquera, V. *J. Appl. Polym. Sci.* **2013**, *129*, 822.
10. Gupta, V. K.; Karar, P. K.; Ramesh, S.; Misra, S. P.; Gupta, A. *Int. J. Res. Pharm. Sci.* **2010**, *1*, 163.
11. Huynh, D. P.; Nguyen, M. K.; Pi, B. S.; Kim, M. S.; Chae, S. Y.; Lee, K. C.; Kim, B. S.; Kim, S. W.; Lee, D. S. *Biomaterials* **2008**, *29*, 2527.
12. Hu, S.; Niu, M.; Hu, F.; Lu, Y.; Qi, J.; Yin, Z.; Wu, W. *Int. J. Pharm.* **2013**, *441*, 693.
13. Niu, M.; Lu, Y.; Hovgaard, L.; Guan, P.; Tan, Y.; Lian, R.; Qi, J.; Wu, W. *Eur. J. Pharm.* **2012**, *81*, 265.
14. Niu, M.; Lu, Y.; Hovgaard, L.; Wu, W. *Int. J. Nanomed.* **2011**, *6*, 1155.
15. Mao, S.; Bakowsky, U.; Jintapattanakit, A.; Kissel, T. *J. Pharm. Sci.* **2006**, *95*, 1035.
16. Pourhosseini, P. S.; Saboury, A. A.; Najafí, F.; Sarbolouki, M. N. *Biochim. Biophys. Acta* **2007**, *1774*, 1274.
17. Yang, L.; Biswas, M. E.; Chen, P. *Biophys. J.* **2003**, *84*, 509.
18. Rarbach, M.; Kettling, A. U.; Koltermann, A.; Eigen, M. *Methods* **2001**, *24*, 104.
19. Pramanik, A.; Thyberg, P.; Rigler., R. *Chem. Phys. Lipids* **2000**, *104*, 35.
20. Alatorre, M.; Taboada, P.; Hartl, F.; Wagner, T.; Freis, M.; Rodríguez, J. R. *Colloids Surf. B* **2011**, *82*, 54.
21. Jayaraman, V.; Keesey, R.; Madden., D. R. *Biochemistry* **2000**, *39*, 8693.
22. Wu, J. J.; Yarwood, D. R.; Pham, Q.; Sills, M. A. *J. Biomol. Screen.* **2000**, *6*, 463.
23. Chen, P. Z.; Policova, C. R.; Pace-Asciak, C. R.; Neumann, A. W. *J. Pharm. Sci.* **1999**, *88*, 1293.
24. Desbrières, J.; Martinez, C.; Rinaudo, M. *Int. J. Biol. Macromol.* **1996**, *19*, 21.
25. Li, J.; Fainerman, B. V.; Miller, R. *Langmuir* **1996**, *12*, 5138.
26. Wang, L.; Atkinson, D.; Small, D. M. *J. Biol. Chem.* **2003**, *278*, 37480.
27. Saulnier, P.; Boury, F.; Malzert, A.; Heurtault, B.; Ivanova, T.; Cagna, A.; Panaïotov, I.; Proust, J. E. *Langumuir* **2001**, *17*, 8104.
28. Miller, R.; Aksenenko, E. V.; Fainerman, V. B. *J. Colloid Interface Sci.* **2001**, *236*, 35.
29. Bogaert, R. V. D.; Joos, P. *J. Phys. Chem.* **1979**, *83*, 2244.
30. Hiral, A.; Odani, H.; Nakajima, A. *Polym. Bull.* **1991**, *26*, 87.
31. Rinaudo, M.; Dung, P. L.; Gey, C.; Milas, M. *Int. J. Biol. Macromol.* **1992**, *14*, 122.
32. Dung, P. L.; Milas, M.; Rinaudo, M.; Desbrieres, *J. Carbohydr. Polym.* **1994**, *24*, 209.
33. Zhang, C.; Ping, Q.; Zhang, H.; Shen, *J. Eur. Polym. J.* **2003**, *39*, 1629.

34. Ma, P. L.; Lavertu, M.; Winnik, F. M.; Buschmann, M. D. *Biomacromolecules* **2009**, *10*, 1490.

35. Manning, G. S.; Ray, J. *J. Biomol. Struct. Dynamics* **1998**, *16*, 461.

36. Kim, W.; Yamasaki, Y.; Kataoka, K. *J. Phys. Chem. B* **2006**, *110*, 10919.

37. Ball, V.; Winterhalter, M.; Schwinte, P.; Lavalle, P.; Voegel, J. C.; Schaaf, P. *J. Phys. Chem. B* **2002**, *106*, 2357.

38. Prevette, L. E.; Kodger, T. E.; Reineke, T. M.; Lynch, M. L. *Langmuir* **2007**, *23*, 9773.

39. Lee, E.; Lee, J.; Jon, S. *Bioconjugate Chem.* **2010**, *21*, 1720.

40. Ybert, C.; Meglio, J. M. *d. Langmuir* **1998**, *14*, 471.

41. Babaka, V. G.; Boury, F. *Colloids Surf. A* **2004**, *243*, 33.

42. Miller, R.; Fainerman, V. B.; Makievski, A. V.; Krägel, J.; Grigoriev, D. O.; Kazakov, V. N.; Sinyachenko, O. V. *Adv. Colloid Interface Sci.* **2000**, *86*, 39.

43. Miller, R.; Leser, M. E.; Michel, M.; Fainerman, V. B. *J. Phys. Chem. B* **2005**, *109*, 13327.

44. Boonsongrit, Y.; Mueller, B. W.; Mitrevej, A. *Eur. J. Pharm.* **2008**, *69*, 388.

45. Dixit, N.; Zeng, D. L.; Kalonia, D. S. *Int. J. Pharm.* **2012**, *439*, 317.

46. Perez, A. A.; Carrara, C. R.; Carrera, C.; Santiago, L. G.; Rodríguez, J. M. *AlChE J.* **2010**, *56*, 1107.

47. Perez, A. A.; Carrera, C.; Rodríguez, J. M.; Rubiolo, A. C.; Santiago, L. G. *Colloids Surf. B* **2010**, *81*, 50.